Appl Phys B (2009) 95: 105–111
DOI 10.1007/s00340-009-3412-4

Applied Physics B
Lasers and Optics

Photonic crystal slow light waveguides with large delay–bandwidth product

L. Dai · C. Jiang

Received: 2 October 2008 / Revised version: 22 December 2008 / Published online: 28 February 2009

Abstract In this paper, we propose the use of two two-dimensional photonic crystal line defect waveguides for slow light with large delay–bandwidth product (DBP). One includes air rings localized at each side of the line defect and the other modifies the radius and distance of holes at each side of the waveguide. We show that we can achieve a very flat band corresponding to nearly constant group index over a broad frequency range by adjusting the parameters of the structure. We show further that the group velocity dispersion (GVD) can reach a relatively small amount and the DBP can be more than 0.6 for the first waveguide and 0.34 for the second waveguide. Numerical simulation by the finite-difference time-domain (FDTD) method demonstrates the propagation of the broadband pulse.

PACS 42.70.Qs · 42.82.Et

1 Introduction

Slow light, which may find many applications in compact optical delay lines and optical buffers, is the hotspot in the domain of optical communication. In the early stage, many researchers used the quantum interference effect of atomic levels (electromagnetically induced transparency, EIT) [1] to achieve the slowing down of light speed [2], but this method has some obvious disadvantages constrained by the property of the material's absorption lines and does not adapt to practical application. Recently, with the rapid development of photonic crystals (PhCs) [3, 4], which can control the light in a similar way as the properties of electrons are controlled in semiconductors, one can decrease the speed of light through carefully designing the dispersion relation of PhC structures.

Therefore, a lot of PhC structures have been extensively studied, and photonic crystal line defect waveguides are regarded as being promising for achieving slow light. Especially, photonic crystal slow light waveguides are suitable for enhanced light–matter interactions and improving the function of devices including switches and all-optical storage [5]. Meanwhile, this slow light waveguide can offer large bandwidth and wavelength flexibility as discussed in [6].

However, the slow modes usually have very high group velocity dispersion (GVD), which can lead to the degradation of the optical signal. So far, several ways were proposed to solve this problem. In [7] two adiabatic gratings were designed compensating for signal dispersion and giving rise to a constant time delay across bandwidths greater than 100 GHz. In addition to this approach, the dispersion curves could be carefully tailored to obtain the zero group velocity dispersion. In [8, 9] a chirped photonic crystal coupled waveguide was designed where an s-shaped dispersive curve is formed with a zero group velocity dispersion inflection point sandwiched between the negative and positive GVDs. Recently, there are some structures [10–13] designed to achieve a flat band with nearly constant group velocity over a certain wavelength range; meanwhile, a delay–bandwidth product (DBP) could be achieved varying from 0.095 to 0.369, and the bandwidth of 2.5 THz with an average group index of 25 can be achieved in the W2 waveguide [11].

L. Dai · C. Jiang (✉)
State Key Laboratory of Advanced Optical Communication Systems and Networks, Shanghai Jiao Tong University, Shanghai, 200240, China
e-mail: cjiang@sjtu.edu.cn
Fax: +86-21-34204597

L. Dai
e-mail: dailei@sjtu.edu.cn

In this paper, we also make use of two novel waveguide structures to achieve wider bandwidth and larger delay–bandwidth product with less GVD. First, through the use of the plane-wave (PW) method [14], we carefully tailor the dispersion relation of the structure to obtain a very flat band. Through the discussion and analysis of the group velocity and GVD, we can achieve a group index of 25 over the bandwidth of 4.9 THz (corresponding to the frequency of $0.0055(2\pi c/a)$), and a DBP of more than 0.60 for the first waveguide. Due to the complexity of the first waveguide, we propose the second waveguide which may be realized in practice with a group index of 25 and a DBP of more than 0.34. Next, numerical simulation by the finite-difference time-domain (FDTD) method [15, 16] demonstrates the propagation of the broadband pulse in the waveguide with little distortion.

2 Waveguide design

The first two-dimensional (2-D) photonic crystal waveguide system studied in this paper is illustrated in Fig. 1a. It consists of a triangular lattice of low-ε dielectric air holes ($\varepsilon_{\mathrm{L}} = 1.0$) embedded in a high-$\varepsilon$ dielectric material ($\varepsilon_{\mathrm{H}} = 12.25$). The lattice spacing is denoted as a, and the radius of each hole is $R = 0.34419a$. The line defect waveguide is created by missing a row of holes in the center along the x-direction; this is the so-called W1 waveguide and it has been investigated widely before [10]. Meanwhile, we use the rows of air rings with inner radius R_{in} and outer radius R_{out} to take the place of the rows of air holes closest to the line defect waveguide in order to obtain the flat band. We focus our attention on TE modes, which have magnetic fields parallel to the z-axis. The frequency-domain calculations by the PW method reveal a 50% photonic band gap between $\omega_{\mathrm{Min}} = 0.19(2\pi c/a)$ and $\omega_{\mathrm{Max}} = 0.32(2\pi c/a)$.

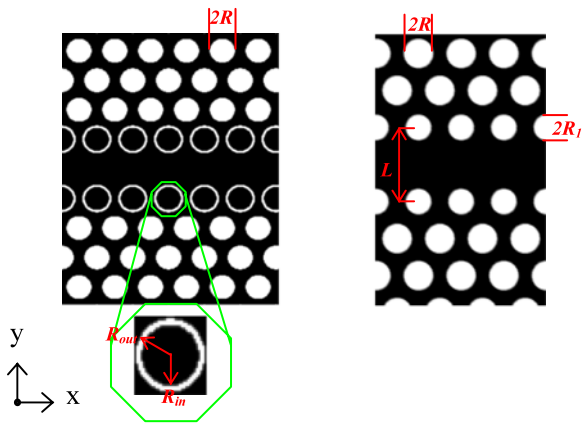

Fig. 1 **a** Schematic of the first structure with a triangular lattice of air holes of radius $R = 0.34419a$, in which the outer radius and inner radius of the ring are R_{out}, R_{in} respectively. **b** Schematic of the second structure with SiO_2 hole radius of $R = 0.34419a$, in which the radius of holes at each side of the waveguide is $R_1 = 0.3a$

We introduce some parameters useful for characterizing the waveguide system. The definition of these parameters is as follows. The first is the group velocity or group index:

$$v_{\mathrm{g}} = \frac{\mathrm{d}\omega}{\mathrm{d}k}, \tag{1}$$

$$n_{\mathrm{g}} = \frac{c}{v_{\mathrm{g}}}. \tag{2}$$

The second are the dispersion parameters including GVD β_2 of the band:

$$\beta_2 = \frac{\mathrm{d}^2k}{\mathrm{d}\omega^2} = -\frac{1}{(\frac{\mathrm{d}\omega}{\mathrm{d}k})^3}\frac{\mathrm{d}^2\omega}{\mathrm{d}k^2} = -\left(\frac{1}{v_{\mathrm{g}}}\right)^3\frac{\mathrm{d}^2\omega}{\mathrm{d}k^2}$$

$$= -\left(\frac{1}{v_{\mathrm{g}}}\right)^2\frac{\mathrm{d}v_{\mathrm{g}}}{\mathrm{d}\omega}. \tag{3}$$

Here ω is the normalized frequency and k is the wave vector. A waveguide with less GVD allows less distortion of a propagating pulse. The delay–bandwidth product (DBP) is defined as [9, 17, 18]

$$\mathrm{DBP} = \tilde{n}_{\mathrm{g}} \cdot \frac{\Delta\omega}{\omega}, \tag{4}$$

where $\tilde{n}_{\mathrm{g}}$ is the average group index [9] and is defined as

$$\tilde{n}_{\mathrm{g}} = \int_{\omega_{\mathrm{o}}}^{\omega_{\mathrm{o}}+\Delta\omega} n_{\mathrm{g}}(\omega)\,\mathrm{d}\omega/\Delta\omega. \tag{5}$$

3 Result and discussion

In this section, we begin by describing the characteristics of guide modes (TE modes) including gap-guide modes and index-guide modes in our waveguide. For gap-guide modes, due to the invariance of the waveguide in the $y = 0$ plane, they can be further classified as y-odd and y-even modes [19]. These modes are demonstrated on the left of Fig. 2 and the field distributions of these modes are shown on the right of Fig. 2 at given points in the band. (Here an H_z field pattern that looks y-even is actually y-odd as H is a pseudo-vector; for a detailed discussion please refer to [19].) From the band diagram we observe that the phenomenon of anti-crossing [20, 21] happen in our waveguide and the y-odd gap-guide mode is very flat between $k = 0.36(2\pi/a)$ and $0.46(2\pi/a)$ due to the interaction between the index-guide mode and the y-odd mode. The anti-crossing is greatly influenced by the structure adjacent to the waveguide. Here we will focus on the influencing of the outer and inner radii

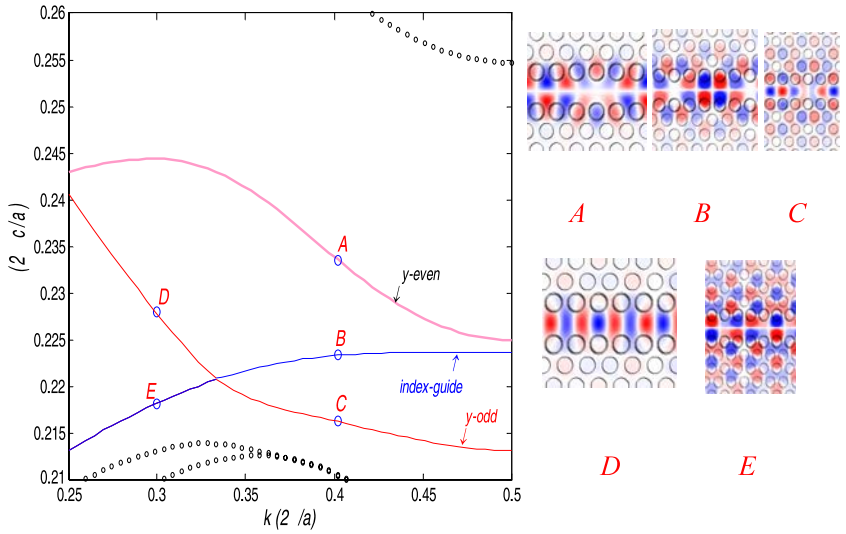

Fig. 2 *Left*: projected band diagram of TE modes for the first waveguide, the guide modes are classified as y even (*solid lines*) or y odd (*dashed lines*). *Right*: field distribution of these bands at given points in *left-hand* figure

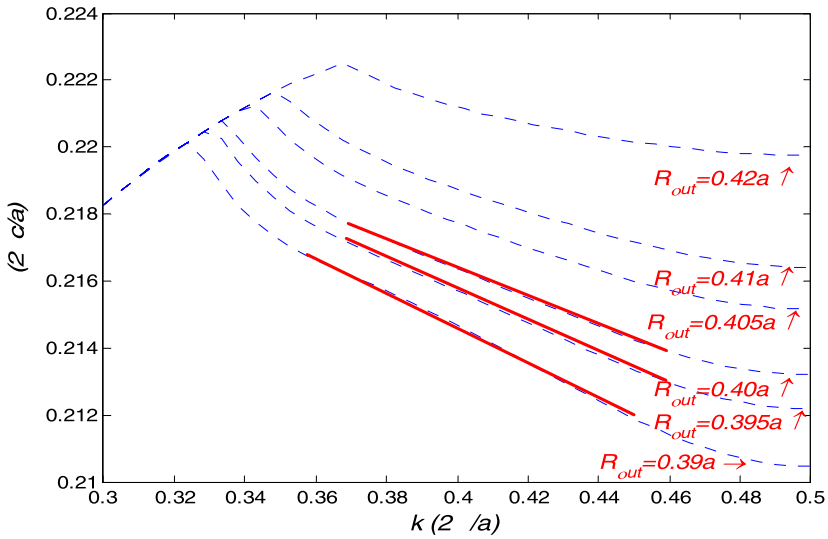

Fig. 3 Dependence of dispersion relation on outer radius of the air ring (R_{out}), where we set $R = R_{\text{in}} = 0.34419a$

of the air ring on the dispersion curve; the result is demonstrated in Fig. 3. The figure depicts the change of the dispersion relation with the outer radius of the air ring, where we set the inner radius of the ring equal to the radius of the air hole.

From the result we observe that the increasing of the outer radius will cause the shift of the dispersion relation to high frequency, as well as the inclination of the curve, decreasing the group velocity. And, the anti-crossing point shifts to bigger wave vector. Furthermore, there are three dispersion curves with nearly flat bands highlighted by the solid red line in the figure between $k = 0.36(2\pi/a)$ and $0.46(2\pi/a)$, especially when the outer radius is $0.40a$. Now, we choose these bands as the research target to investigate the group index, group velocity dispersion and third-order dispersion. Figure 4 illustrates the group index of these flat bands for the outer radii of $0.39a$, $0.395a$ and $0.40a$, respectively. From the result we can note that the group index becomes large with the increasing of the outer radius of the air ring, but the frequency range of the flat region becomes more and more narrow. Next, we further study the GVD of the band for an outer radius of $0.40a$. From the definition of the GVD above, the calculated GVD value is very small due to the constant group index, as can be seen from Fig. 5. The GVD is less than 1 ps/nm/mm within a very wide frequency range. Thus, slow light with nearly constant group index and less GVD can be achieved in very wide bandwidth. The waveguide can achieve, for example, a group index of 25 with less GVD between frequencies of $0.2132(2\pi c/a)$ and $0.2187(2\pi c/a)$ for the outer radius of the ring of $0.40a$.

Even the first waveguide we proposed has very good performance, but it is very difficult to realize in practice due to the existence of the air ring. Thus, the simple slow

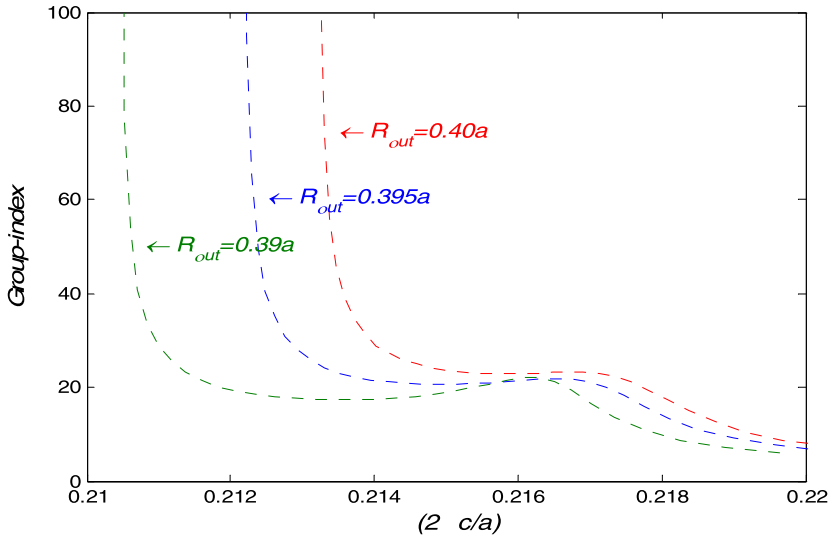

Fig. 4 Group index of flat band as a function of the frequency with different outer radii

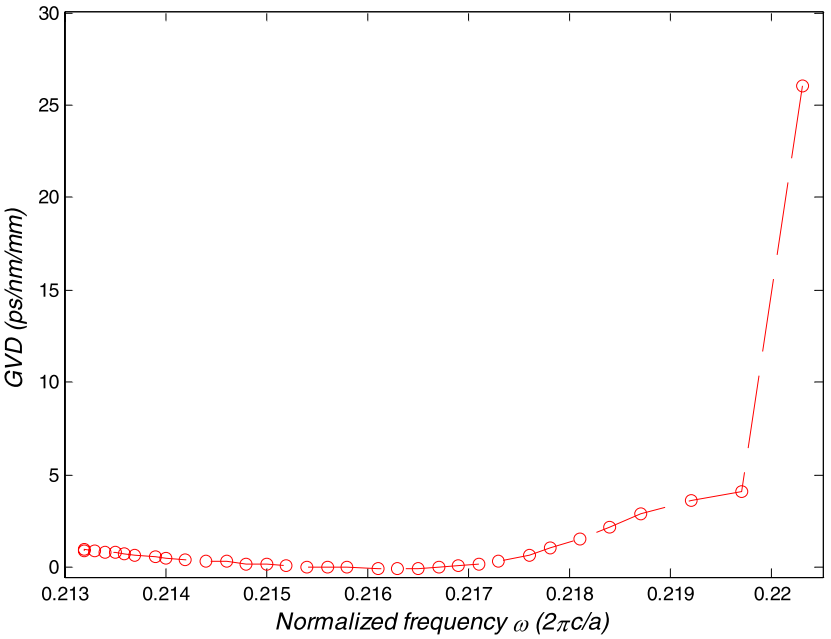

Fig. 5 Group velocity dispersion of the first structure for the outer radius of 0.40a

light waveguide based on the method of anti-crossing should be proposed. This structure is shown in Fig. 1b; it consists of a triangular lattice of low-ε dielectric SiO_2 holes ($\varepsilon_L = 2.25$) with radius of $0.34419a$ embedded in a high-ε dielectric Si material ($\varepsilon_H = 12.25$). This Si–SiO_2 system [22] recently proposed has a 36% photonic band gap between $\omega_{Min} = 0.1898(2\pi c/a)$ and $\omega_{Max} = 0.2735(2\pi c/a)$ and some advantageous features including weakening the perturbations due to surface roughness. The waveguide is shaped the same as the first waveguide but we modify the size of holes at each side of the line defect and set the radius of $0.3a$ unchanged, but in this waveguide the anti-crossing is not going to happen. In order to introduce this phenomenon, we need to adjust the distance between two rows of small holes around the line defect. Finally, we can obtain the anti-crossing with the decreasing of distance. Here we picture the band of the waveguide mode with two parameters $L = 1.692a$ and $L = 1.332a$ as shown in Fig. 6. One describes the intersection of the index-guide mode and the gap-guide mode, and the other depicts the separation of two modes. It is surprising to observe that the flat band is not obtained when the two modes take an anti-crossing, but this flat band can be obtained with the separating of the two modes. This is a completely opposite feature compared with the first waveguide. Next, we further optimize the parameters of the waveguide structure; the bands with different distance L and

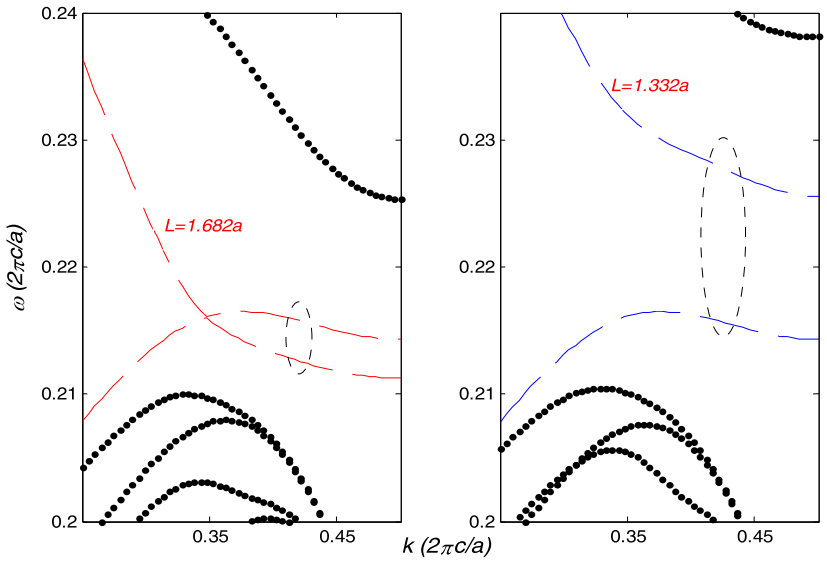

Fig. 6 Projected band diagram of TE mode for the second waveguide, in which we list the band of the waveguide with two parameters $L = 1.692a$ and $L = 1.332a$, respectively

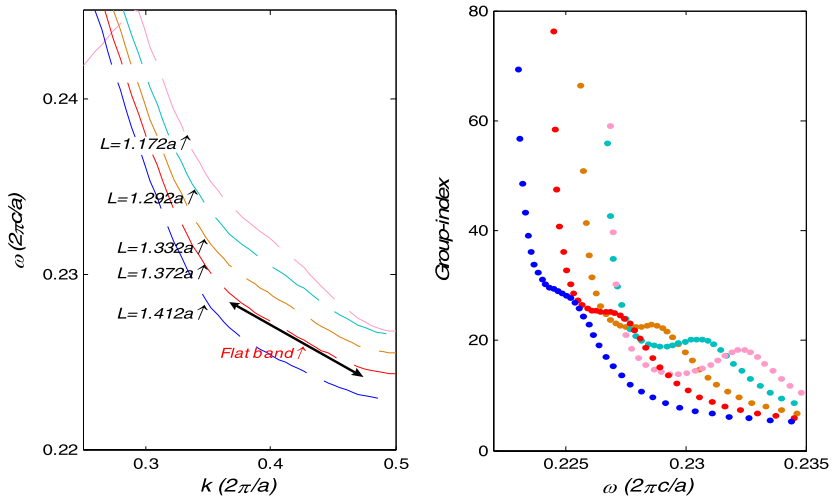

Fig. 7 The band and the corresponding group index with different distances L for the second waveguide

the corresponding group index are shown in Fig. 7. A flat band can be achieved when the distance L is $1.372a$ and we can obtain an average group index of 25 over the frequency range of $0.0031(2\pi c/a)$.

Based on what we learned from the frequency-domain calculation, we can now design a slow light waveguide (here we choose the first waveguide as the simulation target) with optimal parameters for time-domain simulation. Specifically, we perform 2-D FDTD simulation [15] with perfectly matched layer absorbing boundary conditions [16], which solves Maxwell's equations for such a system exactly. Our numerical resolution is 40 pixels/a; we use the waveguide length of $198a$ and the outer radius of the air ring is $0.40a$. At the input of our waveguide system, we launch a Gaussian pulse in time with a carrier frequency of $\omega_0 = 0.216(2\pi c/a)$ and a pulse width of $0.0055(2\pi c/a)$ from the conventional

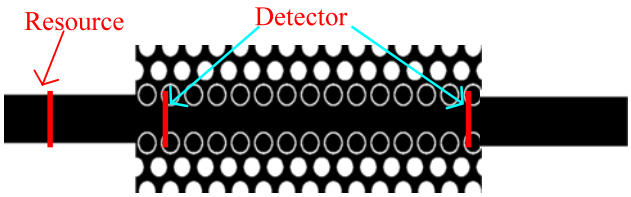

Fig. 8 Schematic of FDTD simulation system of the proposed slow light waveguides

dielectric waveguide into our waveguide. During the simulation, we monitor the field at the input and output ends of the slow light waveguide. The placement of two detectors is shown in Fig. 8.

The final result is demonstrated in Fig. 9. It is clearly noted that the pulse is delayed in the waveguide and the delay time step between two peaks of the pulse is approx-

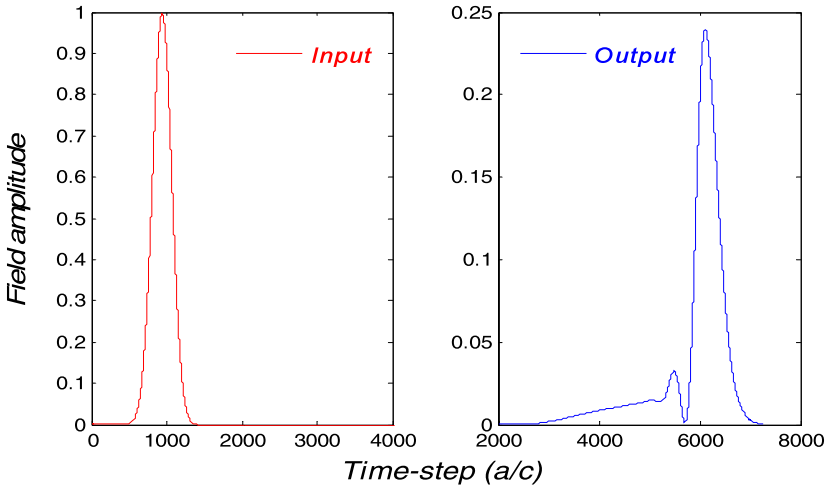

Fig. 9 Field amplitude recorded at the input (*red*) and output (*blue*) ends of the waveguide with the length $198a$, as a function of time, where the center frequency is $0.216(2\pi c/a)$ and the frequency width $0.0055(2\pi c/a)$

imately $4950(a/c)$; thus, the average group index is nearly 25 (group velocity $0.04c$). Due to the GVD in our waveguide being very small but not zero, the shape of the output pulse is slightly broadened compared with the incoming pulse in the frequency width $0.0055(2\pi c/a)$. Meanwhile, we can observe from the result that there is a faster mode with larger group velocity in the waveguide; this is not a surprise because in our photonic crystal waveguide there are two modes (gap-guide mode and index-guide mode) in the frequency range as discussed in Fig. 2. We can increase the length of the waveguide to distinguish the mode with different group velocity. All of the results calculated by the FDTD method essentially coincide with the prediction performed by the PW method.

Before concluding, we estimate quantitative performance characteristics of the slow light waveguide we described. If the operating wavelength $\lambda = 2\pi c/\omega = 1550$ nm lies at the carrier frequency of the Gaussian pulse $0.216(2\pi c/a)$ for the first waveguide, we need the lattice constant of the system to be 335 nm; thus, the frequency width of $0.0055(2\pi c/a)$ (4.9 THz) has a wavelength width of 39 nm ranging from 1529 to 1568 nm. According to the definition of the DBP in (4), we can achieve a large DBP of up to 0.636. And, for the second waveguide we can achieve a DBP of 0.3406; although the performance of the second waveguide is less than the first waveguide, it can be realized in practice more easily.

4 Conclusion

To summarize, we have designed a photonic crystal slow light waveguide with a flat band and very small group velocity dispersion over a frequency width of 4.9 THz, and the delay–bandwidth product can reach more than 0.6. The results calculated by the FDTD method essentially verify the theoretical prediction performed by the PW method. The waveguide will have many important applications in the telecommunication system and nonlinear optics areas.

Acknowledgements This work was supported by the National Natural Science Foundation of China (Grant Nos. 60377023 and 60672017) and the New Century Excellent Talents in University (NCET) Shanghai Optical Science and Technology project (No. 05DZ22009) and sponsored by the Shanghai Pujiang Program.

References

1. K.J. Boller, A. Imamoglu, S.E. Harris, Phys. Rev. Lett. **66**, 2593 (1991)
2. L.V. Hau, Z. Dutton, C.H. Behroozi, S.E. Harris, Nature **397**, 594 (1999)
3. E. Yablonovitch, Phys. Rev. Lett. **58**, 2059 (1987)
4. S. John, Phys. Rev. Lett. **58**, 2486 (1987)
5. M. Soljacic, S.G. Johnson, S. Fan, M. Ibanescu, E. Ippen, J.D. Joannopoulos, J. Opt. Soc. Am. B **19**, 2052 (2002)
6. T.F. Krauss, J. Phys. D: Appl. Phys. **40**, 2666 (2007)
7. M.L. Povinelli, S.G. Johnson, J.D. Joannopoulos, Opt. Express **13**, 7145 (2005)
8. D. Mori, T. Baba, Appl. Phys. Lett. **85**, 1101 (2004)
9. D. Mori, T. Baba, Opt. Express **13**, 9398 (2005)
10. R.J.P. Engelen, Y. Sugimoto, Y. Watanabe, J.P. Korterik, N. Ikeda, N.F. van Hulkst, K. Asakawa, L. Kuipers, Opt. Express **14**, 1658 (2006)
11. M.D. Settle, R.J.P. Engelen, M. Salib, A. Michaeli, L. Kuipers, T.F. Krauss, Opt. Express **15**, 219 (2006)
12. A. Saynatjoki, M. Mulot, J. Ahopelto, H. Lipsanen, Opt. Express **15**, 8323 (2007)
13. J. Li, T.P. White, L. O'Faolain, A. Gomez-Iglesias, T.F. Krauss, Opt. Express **16**, 6227 (2008)
14. S.G. Johnson, J.D. Joannopoulos, Opt. Express **8**, 173 (2001)
15. S.G. Johnson, J.D. Joannopoulos, FDTD software: http://ab-initio.mit.edu/meep
16. A. Taflove, S.C. Hagness, *Computational Electrodynamics: The Finite-Difference Time-Domain Method*, 2nd edn. (Artech House, Norwood, 2000)

17. G. Lenz, B.J. Eggleton, C.K. Madsen, R.E. Slusher, IEEE J. Quantum Electron. **37**, 525 (2001)
18. Z. Wang, S. Fan, Phys. Rev. E **68**, 066616 (2003)
19. J.D. Joannopoulos, S.G. Johnson, J.N. Winn, R.D. Meade, *Photonic Crystals Molding the Flow of Light*, 2nd edn. (Princeton University Press, Princeton, 2008)
20. M. Notomi, Phys. Rev. B **62**, 10696 (2000)
21. S. Olivier, M. Rattier, H. Benisty, C. Weisbuch, C.J.M. Smith, R.M. De La Rue, T.F. Krauss, U. Oesterle, R. Houdre, Phys. Rev. B **63**, 113311 (2001)
22. T.P. White, L. O'Faolain, J. Li, L.C. Andreani, T.F. Krauss, Opt. Express **16**, 17076 (2008)